ELSEVIER

Ceramics International 30 (2004) 765–772

CERAMICS INTERNATIONAL

www.elsevier.com/locate/ceramint

Sintering behavior, mechanical and electrical properties of lead zirconate titanate/NiO composites from coated powders

Ping-Hua Xiang*, Xian-Lin Dong, Chu-De Feng, Ni Zhong, Jing-Kun Guo

Shanghai Institute of Ceramics, Chinese Academy of Sciences, 1295 Ding-Xi Road, Shanghai 200050, PR China

Received 22 July 2003; received in revised form 14 August 2003; accepted 12 September 2003

Available online 10 March 2004

Abstract

High strength NiO-dispersed lead zirconate titanate (PZT) composites are successfully fabricated from NiO nanoparticle-coated PZT powders. Addition of NiO to a PZT matrix does not result in unexpected reaction phase, and some NiO is dissolved in PZT lattice. Microstructural observations reveal that fine NiO particles are homogeneously dispersed at the matrix boundaries and the matrix grain size is refined. Fracture strength of PZT/7.4 vol.% NiO composite is 1.9 times higher than that of monolithic PZT, and fracture toughness (K_{IC}) increases to 1.87 MPa $m^{1/2}$. The electrical properties of PZT/NiO composites increase or are not degraded dramatically with improving mechanical properties.

Keywords: B. Composites; C. Electrical properties; C. Mechanical properties; D. PZT

1. Introduction

Lead zirconate titanate, $Pb(Zr_xTi_{1-x})O_3$ (PZT), and its related materials exhibit excellent piezoelectric properties; hence PZT related ceramics are widely used in the applications such as sensors, transducers, and actuators. However, piezoelectric materials suffer from low mechanical properties and the resulting low electrical reliability [1–4]. For example, fracture strength and fracture toughness of these materials are lower than 100 MPa and 1.0 MPa $m^{1/2}$, respectively. For further high-power applications used under severe circumstances, their poor mechanical and electrical reliability become a critical limitation on the application of these materials. Especially in multilayer piezoelectric actuators, the high electric driving field needed to produce a large displacement may cause mechanical and electrical degradation. Thus, improving mechanical properties of PZT-based materials is worthwhile.

In the past few years, a few studies have dealt with improving mechanical properties of PZT ceramics by adding SiC whiskers [5] or ZrO_2 fibers [6]. Nevertheless, the electrical characteristics are deteriorated with enhancement in mechanical properties. Therefore, it is necessary to design the microstructure possessing excellent mechanical properties without dramatically degrading of electrical properties. Niihara [7] has reported that mechanical properties could be significantly improved by incorporating submicron and nanosized second phases in a brittle ceramic matrix. Recently, this novel design idea has been applied in the field of functional ceramics. Many researchers have reported high mechanical properties and electrical reliability in PZT-based composites. PZT/Ag [8], PZT/Al_2O_3 [9], PZT/Y_2O_3 [10], PZT/In_2O_3 [11] are typical examples. However, the control of the microstructure of PZT composite is difficult to obtain by conventional techniques involving mechanical mixing of ceramic powders and second phase particles. In recent years, powder coating technique has been investigated for preparing homogeneous ceramics. It not only improves the sintering activity and densification, but also enhances the microstructural homogeneity and mechanical properties of sintered body [12,13].

In the present study, we try to fabricate PZT/NiO composites from NiO nanoparticle-coated PZT powders. NiO is expected to be a phase compatible to PZT matrix. The effects of NiO addition on the sintering behavior, mechanical and electrical properties of the PZT/NiO composites have been investigated.

* Corresponding author. Tel.: +86-21-52412023; fax: +86-21-52413903.
E-mail address: phxiang@yahoo.com.cn (P.-H. Xiang).

0272-8842/$30.00
doi:10.1016/j.ceramint.2003.09.012

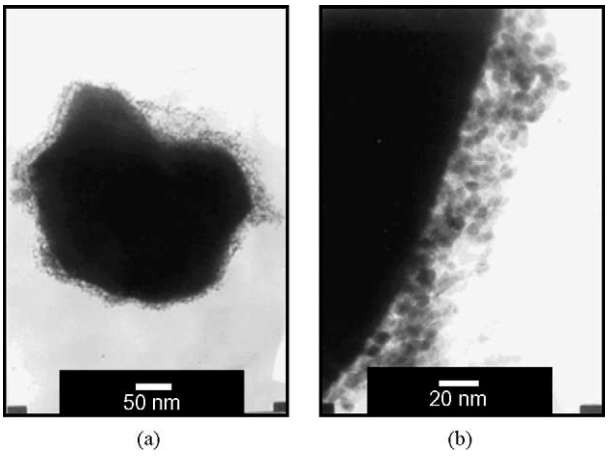

Fig. 1. (a) TEM image of NiO nanoparticle-coated PZT powder, (b) higher-magnification TEM image of PZT/NiO region [14].

2. Experimental procedure

PZT/NiO composites were fabricated from NiO nanoparticle-coated PZT powders obtained by the heterogeneous precipitation method [14]. The starting PZT powder had a composition of $Pb(Zr_{0.52}Ti_{0.48})O_3$ and the average particle size was 0.36 μm. As shown in Fig. 1, NiO particles with the size of about 8 nm were spherical and weakly agglomerated coating on PZT particle. The coated powders were uniaxially pressed in the form of disc shape (∅ 11 mm × 2 mm) and rectangle shape (42 mm × 42 mm × 8 mm) at a pressure of 40 MPa and subsequently followed by cold isostatic pressing (CIP) at 200 MPa. After CIPing, the pressed samples were sintered at 1100–1260 °C for 1.5 h in a Pb-rich atmosphere controlled by the sintered PZT ceramic powder which is available to reduce the lead loss in the specimens. For electrical measurements, Ag paste was painted on both sides of the discs and then fired at 650 °C for 30 min. For mechanical measurements, the standard bars (36 mm × 4 mm × 3 mm) were cut from the sintered bodies and one of the major faces (dimensions of 36 mm × 4 mm) was polished with diamond paste to obtain mirror surface.

For sintered sample phase characterization, X-ray diffraction pattern was obtained using an automated dffractometer (Rigaku RAX-10, Japan) with Cu Kα1 radiation. The content of NiO was determined by inductively coupled plasma atomic emission spectrometry (ICP-AES) (Varian Vista AX, USA). The bulk density was determined by using the Archimedes method in water. Fracture strength was measured on the standard bars by three-point bending method (INSTRON 8501, UK). The span was 30 mm and the rate of loading was 0.5 mm/min. Hardness and fracture toughness was measured by the indentation fracture (IF) technique [15] using a micro-Vickers diamond indenter (AKASHI AVK-A, Japan). The indentation load of 49 N was applied for 15 s. The grain boundary of the composites was revealed by etching with a dilute solution of HCl and HF. The microstructure was analyzed by field emission scanning electron microscope (JSM-6700F, JEOL, Japan). The size of NiO particles and the average of PZT grain size were determined by the linear intercept method from the SEM image of the surfaces of the etched samples. For piezoelectric properties, the specimens were poled in silicon oil at 120 °C for 20 min under the electric field of 2.5 kV/mm. The dielectric constants were measured at 1 kHz and electromechanical coupling factors (k_p), Young's modulus were measured by the resonance and antiresonance method using the HP4294A impedance analyzer.

3. Results and discussion

3.1. Phase characterization of PZT/NiO composites

X-ray diffraction patterns of the monolithic PZT and PZT/NiO composites sintered at 1220 °C for 1.5 h are shown in Fig. 2. The XRD analysis reveals that the PZT matrix is a ferroelectric tetragonal phase, regardless of the volume fraction of NiO. All the peaks are identified as PZT and NiO with cubic phase. No reaction phases between the PZT matrix and NiO addition is found in XRD patterns. The relative intensity of NiO phase peaks for PZT/7.4 vol.% NiO composite is higher than that of the PZT composite with 3.6 vol.% NiO addition, which indicates that NiO is a compatible phase to the PZT matrix. There is no NiO detected in the PZT composites with 0.9 and 1.7 vol.% NiO addition. However, due to the detection limit of the XRD analysis, whether small amount of NiO diffuses toward PZT matrix or not cannot be concluded from the XRD patterns.

The variation of tetragonality (c/a) of PZT composites with NiO content is shown in Fig. 3. The value of PZT/NiO composite is lower than that of monolithic PZT. The grain size and the solution of NiO in PZT are two factors affecting

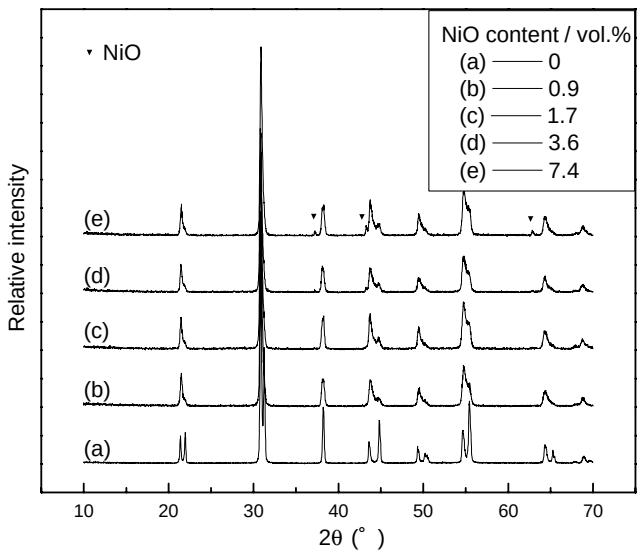

Fig. 2. X-ray diffraction patterns for the monolithic PZT and PZT/NiO composites with x vol.% NiO.

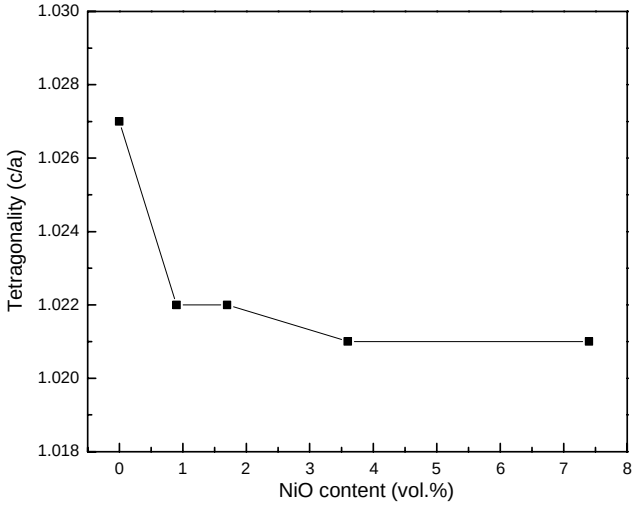

Fig. 3. Variation of tetragonality (c/a) of the PZT composites with NiO content.

the tetragonality (c/a). Arlt et al. [16] have reported that c/a ratio decreased with the reduction of grain size when the grain size is smaller than 1 μm. As shown in Fig. 6, the average grain size of PZT/NiO composite is larger than 1 μm. Therefore, the major factor to reduce the tetragonality (c/a) is attributed to the solution of NiO in PZT matrix. It is well known that PZT system has an ABO_3-type perovskite structure. The A-sites are occupied by Pb^{2+} ions and the B-sites by Zr^{4+} and Ti^{4+} ions. A dopant can go either to the A- or B-site, its distribution on the two sites being a function of the valence and ionic radius of the dopant. The ionic radius of Ni^{2+} ion (0.069 nm) is almost equal to that of B-site cations: Zr^{4+} (0.072 nm) and Ti^{4+} (0.0605 nm). Although the valence of Ni^{2+} ion is the same as that of A-site cation: Pb^{2+}, the ionic radius of Ni^{2+} is much smaller than that of Pb^{2+} (0.119 nm) [17]. It might be expected that Ni^{2+} ion prefer to enter into B-site in perovskite structure. A Ni^{2+} ion substitution will create an oxygen vacancy to compensate charge neutrality. The distortion of oxygen octahedron structure results in the variation of tetragonality (c/a). However, there is little change in the tetragonality (c/a) of PZT composites when the content of NiO is higher than 0.9 vol.%. Furthermore, there are some NiO particles appearing in PZT/0.9 vol.% NiO composite (Fig. 9b). Therefore, it can be estimated that the solubility of NiO in PZT matrix is lower than 0.9 vol.%.

3.2. Sintering behavior and microstructure of PZT/NiO composites

The NiO nanoparticle-coated PZT powders were sintered at various temperatures. Fig. 4 shows the densification curves of the monolithic PZT and PZT/NiO composites. It reveals that the coated powders could be sintered to above 96% of the theoretical density even at a temperature as low as 1200 °C. The relative density of composites sintered

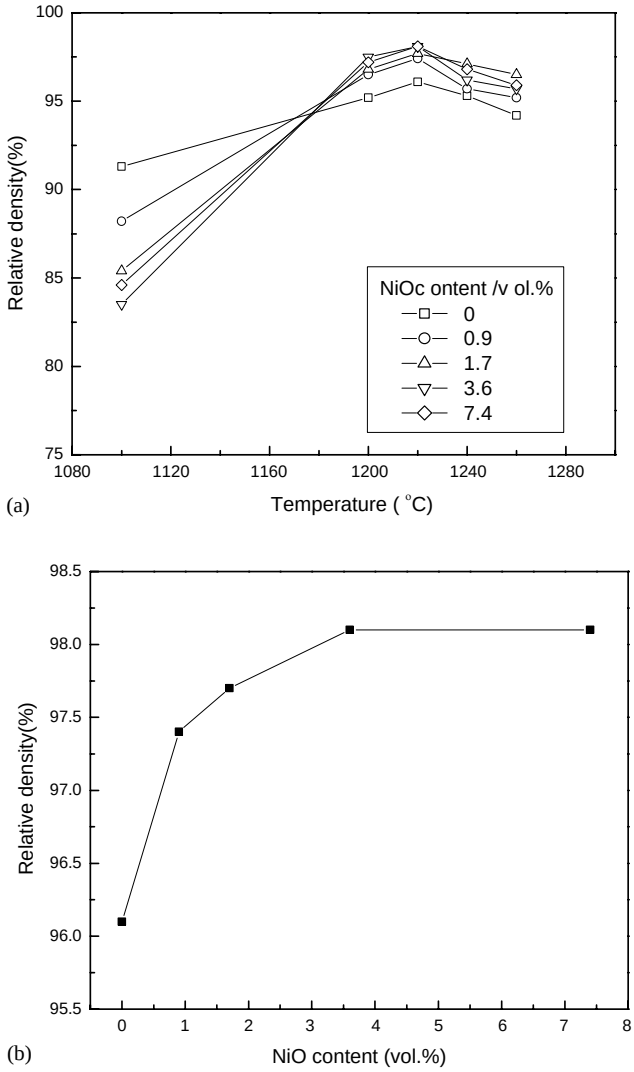

Fig. 4. Variation of relative density of the monolithic PZT and PZT/NiO composites (a) with sintering temperature and (b) with NiO content sintered at 1220 °C.

at 1220 °C for 1.5 h increase with the content of NiO, as shown in Fig. 4b. These observations show the benefit of coated powders during sintering process. The same behavior has been reported in the ceramic–ceramic composites prepared from their corresponding coated powders [11,18]. This sintering behavior can be associated with the high reactivity of nanoparticles in the coating layers. Moreover, the formation of oxygen vacancies due to Ni^{2+} ion substitution in the perovskite structure is considered to be another reason responsible for the sintering behavior of PZT/NiO composites. The oxygen vacancies accelerate mass transfer and densification, which result in high relative density [8].

Fig. 5 shows the SEM photographs of surface of the monolithic PZT and PZT/7.4 vol.%NiO composites sintered at 1220 °C for 1.5 h. The dark gray phases in Fig. 5b are NiO particles which homogeneously dispersed in PZT matrix. The NiO particles are surrounded by three or more matrix grains. The size of NiO particle and the average grain

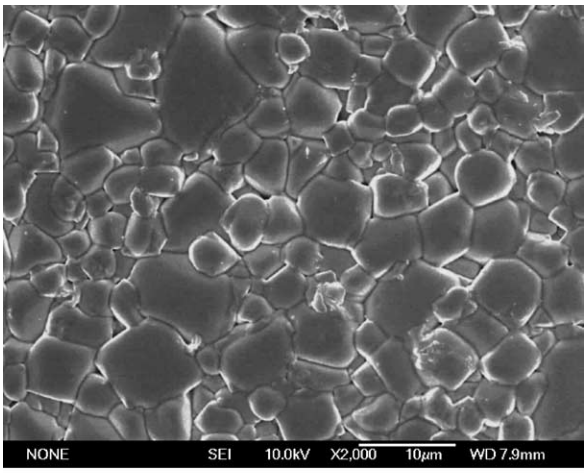

Fig. 5. SEM photographs of the surface of (a) the monolithic PZT and (b) PZT/NiO composites with 7.4 vol.% NiO addition.

size of PZT matrix are shown as a function of NiO content in Fig. 6. The NiO particles grow slightly with increasing NiO content. The particle size increases from about 1.0 μm with 0.9 vol.% NiO addition to 1.3 μm with 7.4 vol.% NiO addition, whereas, that in the starting coated PZT powders is only 8 nm. It is obvious that NiO nanoparticles appear to agglomerate and grow during sintering process. This means that NiO nanoparticles, initially coating on the surface of PZT powder, move along grain boundaries and gradually concentrate at the boundary intersections, and agglomerate into larger particles during the grain growth of the matrix. That is, the growth of NiO particles occurs by coalescence. The average PZT grain size decreases obviously after doping NiO addition. The value decreases from 4.5 to 1.3 μm with an addition of 0.9 vol.% NiO and shows no obvious change with the further increasing the content of NiO addition. Tzing et al. [19] have reported that both the Ni solute and NiO second phase can inhibit the grain growth of $BaTiO_3$ matrix. In the present study, the average grain sizes of PZT matrix vary little with increasing NiO content above 0.9 vol.%. Therefore, the contribution to inhibiting the grain growth by NiO second phase is small. It is likely that the NiO particles move along the grain boundaries, offering little inhibition to the growth of PZT matrix during sintering process.

3.3. Mechanical properties of PZT/NiO composites

The variation of hardness and Young's modulus with NiO content are shown in Fig. 7. Hardness and Young's modulus increase with increasing NiO content. As stated previously, some Ni^{2+} ion may incorporate into the perovskite structure. Ni^{2+} ions substitution for B-site ions produces oxygen vacancies in the structure. It is well known that oxygen vacancies in the perovskite structure generally result in typical

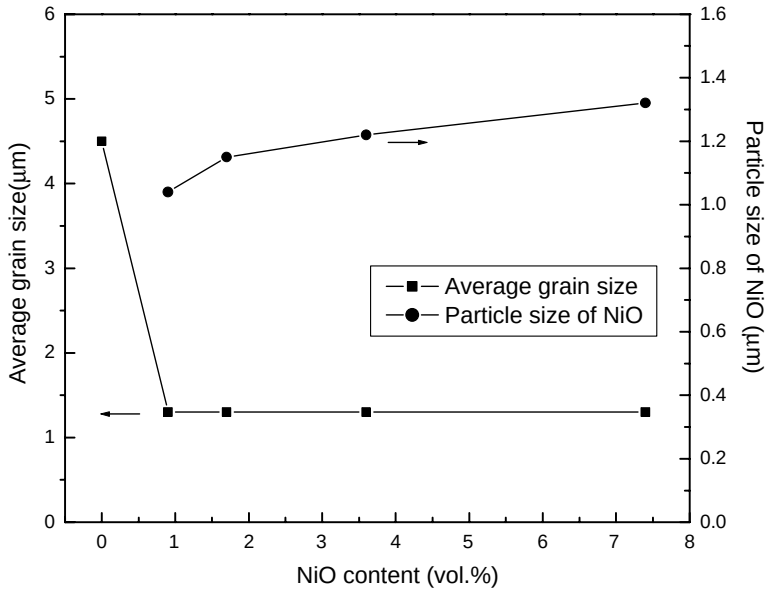

Fig. 6. Variation of the size of NiO particle and the average PZT grain size for PZT/NiO composites with NiO content.

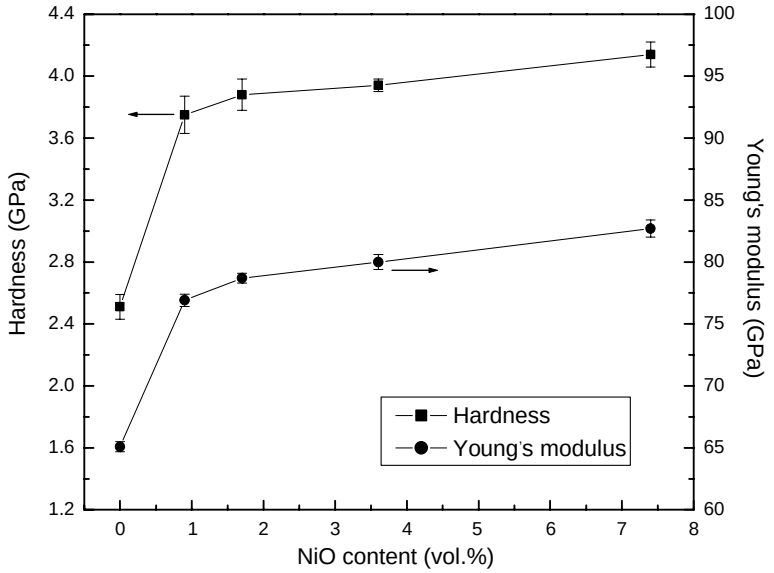

Fig. 7. Variation of hardness and Young's modulus for the monolithic PZT and PZT/NiO composites with NiO content.

"hard" properties of ferroelectric ceramics: high hardness, elastic modulus and mechanical quality factor. Thus, the creation of oxygen vacancies due to Ni^{2+} ion substitution is considered to be a possible reason responsible for the high hardness and Young's modulus observed in Fig. 7. Although the solubility limit of NiO in perovskite structure is less than 0.9 vol.%, as mentioned above, the values of hardness and Young's modulus still increase slightly with further increasing NiO content above 0.9 vol.%, which can be explained by the higher hardness and Young's modulus of NiO than those of PZT matrix.

Fig. 8 shows the variation of fracture toughness (K_{IC}) values with NiO content. The K_{IC} of PZT/NiO composites decreases with 0.9 vol.% NiO addition. Further increasing the content of NiO above 0.9 vol.%, K_{IC} increases from 1.55 to 1.87 MPa $m^{1/2}$ with an addition of 7.4 vol.% NiO. The most probable mechanism responsible for the enhancement in fracture toughness is the crack deflection due to the interaction between PZT matrix and NiO particles. SEM images of the crack traces induced by the Vickers indentation on the surface of the monolithic PZT and PZT/NiO composites are illustrated in Fig. 9. In the monolithic PZT, the crack mainly passes through the interface of PZT grains (Fig. 9a). For the PZT/0.9 vol.% NiO composites, the major crack propagate into the matrix grains in a straight line, selecting the nearest-neighbor grains (Fig. 9). The small reduction in fracture toughness of PZT composite with 0.9 vol.% NiO addition results from the decrease in crack

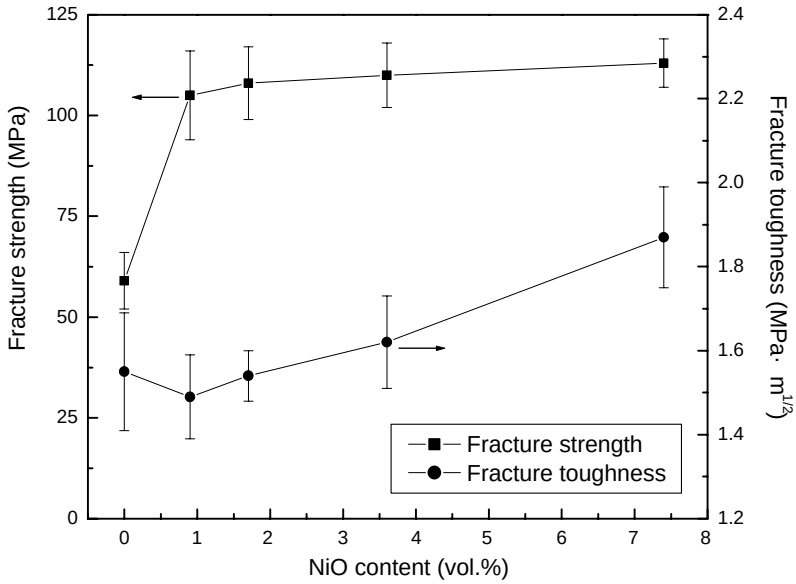

Fig. 8. Variation of fracture strength and fracture toughness for the monolithic PZT and PZT/NiO composites with NiO content.

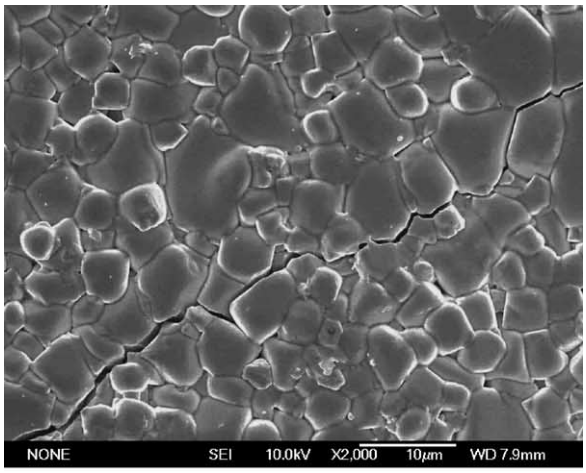

(a)

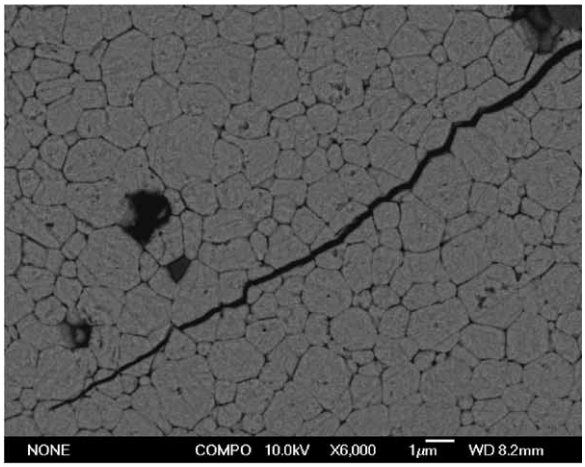

(b)

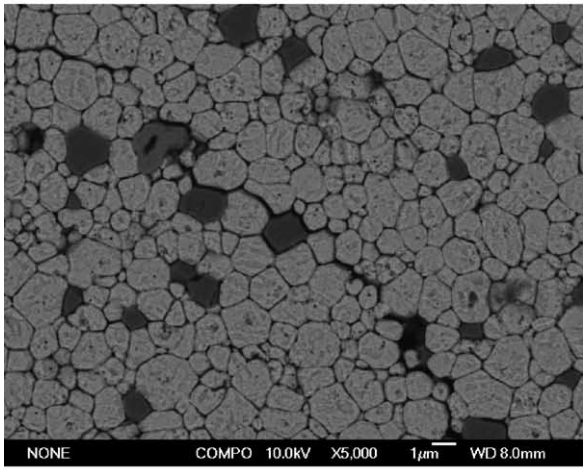

(c)

Fig. 9. SEM photographs of the crack propagation in (a) the monolithic PZT and PZT/NiO composites with (b) 0.9 vol.% NiO, (c) 7.4 vol.% NiO addition.

deflection. However, in the PZT/7.4 vol.% NiO composite, the crack front never propagates in a straight line, but rather is deflected, and mainly propagates along the interface between the matrix and NiO particles (Fig. 9c). The change in crack propagation can be considered to be influenced by the thermal internal stresses caused by the thermal expansion mismatch between the matrix and the NiO particles. Because the thermal expansion coefficients of the PZT matrix and NiO particles are 13×10^{-6} and $17.1 \times 10^{-6}\,^{\circ}\mathrm{C}^{-1}$, respectively [20,21], the considerable amounts thermal residual stresses are generated in the matrix grains and the NiO particles during the cooling process from the sintering temperature. The residual stress values of some composites can be calculated by the expression derived by Selsing [22]:

$$\sigma = \frac{\Delta\alpha\Delta T}{(1+\nu_{\mathrm{m}}/2E_{\mathrm{m}}) + (1-2\nu_{\mathrm{p}}/E_{\mathrm{p}})} \tag{1}$$

where $\Delta\alpha$ is the difference in the thermal expansion coefficients between the matrix and the particle, ΔT is the temperature change; E and ν are the Young's modulus and Poisson's ratio, respectively (the subscripts "m" and "p" denote the matrix and particle, respectively). In the present case, the values of 262.9 GPa and 0.37 are selected for Young's modulus and Poisson's ratio of NiO, respectively [21]. The measured Young's modulus and Poisson's ratio for PZT matrix via the resonance and antiresonance method are 65.1 GPa and 0.39. Substituting values for E and ν into Eq. (1) gives a value to be ~420 MPa in tension in the radial direction and ~210 MPa in compression in the tangential direction at the PZT matrix/NiO particle interface. The thermal residual stresses induce the propagation of crack to bypass the NiO particles. Consequently, the crack deflection leads to the toughening of the composites with larger NiO volume fraction.

Fracture strength is also shown in Fig. 8. The fracture strength increases remarkably from 59 to 105 MPa with 0.9 vol.% addition. Further increasing the content of NiO above 0.9 vol.%, the fracture strength increases a little. The observed strength variation coincides with the change of the average grain size of PZT/NiO composite (Fig. 6). It is well known that the reduction of matrix grain size would result in the strengthening of composites owning to the reduction of critical flaw size [23]. For brittle materials (such as ceramics), the fracture strength can be defined by the following equation:

$$\sigma_{\mathrm{f}} = \frac{K_{\mathrm{IC}}}{Y\sqrt{c}} \tag{2}$$

where K_{IC}, Y and c represent the fracture toughness, the geometrical parameter of a flaw and one-half of the width of the initial flaw, respectively. In general, c is proportional to the grain size in dense polycrystalline materials. Therefore, the improvement of fracture strength can be attributed to the refinement of the matrix grain. According to Eq. (2), the strength ratio of two polycrystalline materials can be related by average grain size ratio if the toughness values of the specimens are the same. In the present study, the K_{IC} values of PZT/1.7 vol.% NiO composite is almost the

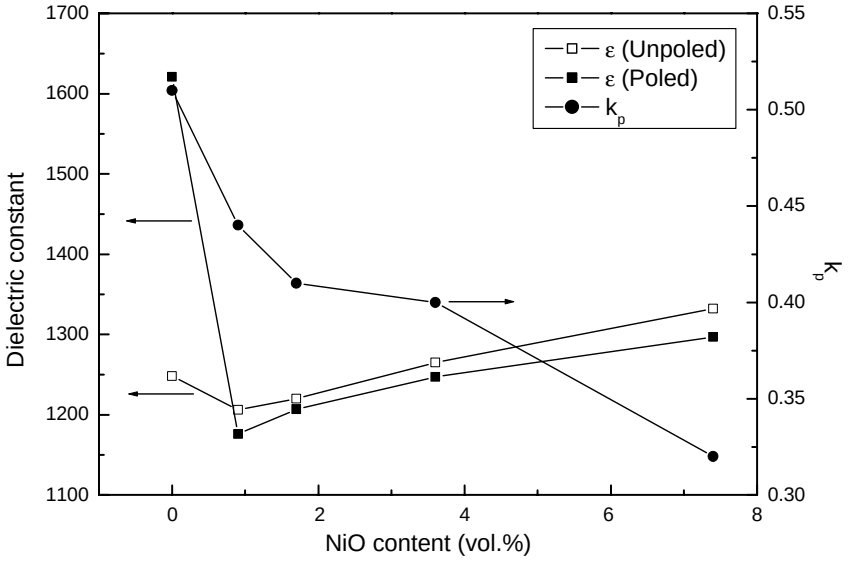

Fig. 10. Variation of dielectric constant, and planar electromechanical coupling factors, k_p, for the monolithic PZT and PZT/NiO composites with NiO content.

same as that of the monolithic PZT (Fig. 8). The average grain size ratio predicts 86% of the strength increment for the PZT/1.7 vol.% NiO composite, which matches very well with the experimental value (83%).

3.4. Electrical properties of PZT/NiO composites

The dielectric constant of composites as a function of NiO content at room temperature is shown in Fig. 10. The dielectric constant of the unpoled and poled samples decrease with increasing amounts of NiO up to 0.9 vol.% and thereafter increase up to 7.4 vol.%. However, the dielectric constant of the poled PZT increases obviously after poling, whereas, that of PZT/NiO composites shows a small reduction after poling. These observations suggest that domain switching caused by the poling is prevented by doping NiO addition. Moreover, the average grain sizes of PZT/NiO composites are reduced to 1.3 μm. Thus, the domain clamping due to the reduction of grain size [24] is considered to be another reason responsible for the low dielectric constant of the composites after poling.

The variation of planar electromechanical coupling factors, k_p, with NiO content is also shown in Fig. 10. k_p decrease with increasing the content of NiO. It is generally accepted that the domain clamping will lead to lower saturation polarization and thus results in reduction in k_p. For PZT/NiO composites, the reduction in k_p can be attributed to the domain clamping caused by the formation of oxygen vacancies [25] due to the substitution of Ni^{2+} ion in perovskite structure and by the reduction of grain size, as mentioned above. In addition, the non-ferroelectric NiO second phase in PZT matrix also causes the fall in k_p. Although, the values of k_p of composites decrease, PZT composites (NiO content lower than 3.6 vol.%) show suitable k_p values (higher than 0.40) for piezoelectric actuator.

4. Conclusions

The present work has shown that high strength PZT composites containing fine NiO particles can be obtained from NiO nanoparticle-coated PZT powders. SEM observations reveal that the NiO particles are located at the matrix grain boundaries and the microstructure of the matrix is refined. The microstructure strongly influences the mechanical and electrical properties of the PZT/NiO composites. Fracture strength of 7.4 vol.% NiO added PZT composite was 1.9 times higher than that of monolithic PZT and the fracture toughness increased to 1.87 MPa $m^{1/2}$. The crack deflection due to the thermal residual stresses results in the toughening of the material. The electrical properties of the composites are improved or not reduced dramatically with the high mechanical properties. As a consequence, the PZT/NiO composite (NiO content lower than 3.6 vol.%) shows good mechanical and suitable piezoelectric properties for high reliable ceramic actuators.

References

[1] S.R. Winzer, N. Shankar, A.P. Ritter, Designing cofired multilayer electrostrictive actuator for reliability, J. Am. Ceram. Soc. 72 (1989) 2246–2257.
[2] G.S. White, A.S. Raynes, M.D. Vaudin, S.W. Freiman, Fracture behavior of cyclically loaded PZT, J. Am. Ceram. Soc. 77 (1994) 2603–2608.
[3] T. Sakai, M. Ishikiriyama, R. Shimazaki, Durability of piezoelectric ceramics for an actuator, Jpn. J. Appl. Phys. 31 (1992) 3051–3054.
[4] R. Fu, T.Y. Zhang, Effects of an electric field on the fracture toughness of poled lead zirconate titanate ceramics, J. Am. Ceram. Soc. 83 (2000) 1215–1218.
[5] T. Yamamoto, H. Igarashi, K. Okazaki, Electrical and mechanical properties of SiC whisker reinforced PZT ceramics, Ferroelectrics 63 (1985) 281–288.

[6] M. Takahashi, K. Baba, O. Nishizato, A. Takamura, M. Katsube, Mechanical and electromechanical properties of monoclinic ZrO_2 fiber/PZT composites, J. Ceram. Soc. Jpn. 102 (1994) 63–68.
[7] K. Niihara, New design concept of structural ceramics—ceramic nanocomposites, J. Ceram. Soc. Jpn. 99 (1991) 974–982.
[8] H.J. Hwang, M. Yasuoka, M. Sando, M. Toriyama, Fabrication, sinterability, and mechanical properties of lead zirconate titanate/silver composites, J. Am. Ceram. Soc. 82 (1999) 2417–2422.
[9] K. Tajima, H.J. Hwang, M. Sando, Electric-field-induced crack growth behavior in PZT/Al_2O_3 composites, J. Am. Ceram. Soc. 83 (2000) 651–653.
[10] P.H. Xiang, X.L. Dong, H. Chen, Z. Zhang, J.K. Guo, Mechanical and electrical properties of small amount of oxides reinforced PZT ceramics, Ceram. Int. 29 (2003) 499–503.
[11] P.H. Xiang, X.L. Dong, C.D. Feng, H. Chen, Y.L. Wang, Microstructure and mechanical properties of small amounts of In_2O_3 reinforced $Pb(Zr_xTi_{1-x})O_3$ ceramics, Mater. Res. Bull. 38 (2003) 1147–1154.
[12] C.M. Wang, F.L. Riley, Alumina-coating of silicon nitride powder, J. Eur. Ceram. Soc. 10 (1992) 83–93.
[13] W.H. Tuan, H.H. Wu, T.J. Yang, The preparation of Al_2O_3/Ni composites by a powder coating technique, J. Mater. Sci. 30 (1995) 855–859.
[14] P.H. Xiang, X.L. Dong, C.D. Feng, Y.L. Wang, Fabrication of NiO nanoparticle-coated lead zirconate titanate powders by the heterogeneous precipitation method, J. Am. Ceram. Soc. 86 (2003).
[15] K. Niihara, R. Morena, D.P.H. Hasselman, Evaluation of K_{IC} of brittle solids by the indentation method with low crack-to-indent ratios, J. Mater. Sci. Lett. 1 (1982) 13–16.
[16] G. Arlt, D. Hennings, G. de With, Dielectric properties of fine-grained barium titanate ceramics, J. Appl. Phys. 58 (1985) 1619–1625.
[17] R.D. Shannon, Revised effective ionic radii and systematic studies of interatomic distances in halides and chalcogenides, Acta Crystallogr. A32 (1976) 751–767.
[18] T.D. Mitchell Jr., L.C. De Jonghe, Processing and properties of particulate composites from coated powders, J. Am. Ceram. Soc. 78 (1995) 199–204.
[19] W.H. Tzing, W.H. Tuan, H.L. Lin, The effect of microstructure on the electrical properties of NiO-doped $BaTiO_3$, Ceram. Int. 25 (1999) 425–430.
[20] H.J. Hwang, T. Nagai, T. Ohji, M. Yasuoka, M. Sando, M. Toriyama, K. Niihara, Curie temperature anomaly in lead zirconate titanate/silver composites, J. Am. Ceram. Soc. 81 (1998) 709–712.
[21] A. Green, Determination of growth stresses in nickel oxide using X-ray diffraction, Mater. Sci. Technol. 8 (1992) 159–162.
[22] J. Selsing, Internal stresses in ceramics, J. Am. Ceram. Soc. 44 (1961) 419.
[23] R.C. Pohanka, S.W. Freiman, B.A. Bender, Effect of the phase transformation on the fracture behavior of $BaTiO_3$, J. Am. Ceram. Soc. 61 (1978) 72–75.
[24] T. Yamamoto, K. Yamamoto, R. Tanaka, K. Okazaki, T. Ueyama, Ferroelectric properties of $Pb(Zr_{0.53}Ti_{0.47})O_3$ ceramics synthesized by partial oxalate method, Jpn. J. Appl. Phys. 28 (Suppl. 28-2) (1989) 63–66.
[25] A.J. Moulson, J.M. Herbert, Electronic Ceramic Materials and Their Applications, Chapman and Hall, London, 1990.